




Small dome-shaped pigment epithelium detachment in polypoidal choroidal vasculopathy: an under-recognized sign of polypoidal lesions on optical coherence tomography?

Yuwei Wang^{1,2} · Qiyu Bo^{1,2} · Huixun Jia^{1,2} · Mengsha Sun^{1,2} · Yang Yu¹ · Peirong Huang^{1,2} · Jing Wang^{1,2} · Nana Xu^{1,2} · Fenghua Wang^{1,2,3}  · Hong Wang^{1,2,3} · Xiaodong Sun^{1,2,3}

Received: 2 April 2020 / Revised: 27 November 2020 / Accepted: 18 December 2020 / Published online: 8 April 2021
© The Author(s), under exclusive licence to The Royal College of Ophthalmologists 2021

Abstract

Purpose To evaluate the diagnostic accuracy of spectral-domain optical coherence tomography (SD-OCT) and swept-source optical coherence tomographic angiography (SS-OCTA) to identify polypoidal lesions in serous or serosanguinous maculopathy.

Materials and methods A retrospective review of patients presenting pigment epithelial detachments (PEDs) with the diagnosis of polypoidal choroidal vasculopathy (PCV), neovascular age-related macular degeneration (nAMD), and central serous chorioretinopathy (CSC), all of which underwent SD-OCT, SS-OCTA, and indocyanine green angiography (ICGA). Typical features of polypoidal lesions on SD-OCT included sharply peaked PED, notched PED, and hyperreflective ring underneath PED. SS-OCTA feature was vascularized PEDs on cross-sectional images corresponding to cluster-like structures on en face images. The parameters of PEDs were measured for analysis.

Results Of 72 eyes, 30 had PCV, 22 had nAMD, and 20 had CSC. A total of 128 localized PEDs were detected on SD-OCT. Typical features on SD-OCT had a high specificity (94.0%) but a limited sensitivity (73.8%). SS-OCTA features provided a higher sensitivity (96.7%). PEDs of the polypoidal lesions unrecognized by SD-OCT were dome-shaped, with smaller ratio of height to base diameter and less area, and almost had heterogeneous internal reflectivity and a connected double-layer sign. Some lesions misidentified by SS-OCTA developed into ICGA-proven polypoidal lesions at follow-up visits.

Conclusion A small dome-shaped PED with heterogeneous internal reflectivity and a connected double-layer sign on SD-OCT may suggest a polypoidal lesion of PCV. SS-OCTA may be a helpful tool to investigate preclinical PCV and observe the formation of polypoidal lesions.

These authors contributed equally: Yuwei Wang, Qiyu Bo

Supplementary information The online version of this article (<https://doi.org/10.1038/s41433-020-01390-0>) contains supplementary material, which is available to authorized users.

✉ Fenghua Wang
shretina@sjtu.edu.cn

✉ Hong Wang
wanghong700520@126.com

¹ Department of Ophthalmology, Shanghai General Hospital, Shanghai Jiao Tong University School of Medicine, Shanghai, China

² National Clinical Research Center for Eye Diseases, Shanghai, China

³ Shanghai Key Laboratory of Fundus Diseases, Shanghai, China

Introduction

Polypoidal choroidal vasculopathy (PCV) is a macular disease that leads to vision loss, especially in Asia [1]. It is characterized by polypoidal lesions with or without a branching vascular network (BVN) [2, 3]. The identification of polypoidal lesions is essential for the diagnosis of PCV. Moreover, polypoidal lesions are often multiple in the same eye, and it is necessary to detect them as much as possible for both treatment and research. There has been ongoing debate regarding the structure and pathogenesis of polypoidal lesions [4, 5]. And the appearance of them is complex and diverse, with different natural history and treatment responses [6–10], implying that polypoidal lesions need be treated differently. Two separate studies reported that baseline size and location of polypoidal lesions were significantly associated with long-term visual

outcomes after combination therapy for PCV [8, 9]. Another study recommended combined treatment of anti-vascular endothelial growth factor (anti-VEGF) and photodynamic therapy (PDT) for cluster-like polypoidal lesions that had a higher risk of massive submacular hemorrhage [11]. Therefore, identification of polypoidal lesions is necessary not only for the diagnosis of PCV, but also for further research on pathological mechanism and individualized treatment.

Although indocyanine green angiography (ICGA) is currently the gold standard for the diagnosis of PCV, it is invasive, time-consuming, and also causes adverse reactions. In addition, it is not available in some clinical settings [12]. Optical coherence tomography (OCT) has been increasingly recognized as a useful imaging examination for PCV. Highly suggestive features using OCT for the polypoidal lesions include a sharply peaked pigment epithelial detachment (PED), a notched PED, and a hyperreflective ring underneath PED [13–15]. De Salvo et al. [15] showed a sensitivity of 94.6% and a specificity of 92.9% for the above features in diagnosing PCV. However, in clinical practice, we found that some polypoidal lesions shown as small dome-shaped PEDs on OCT are likely under-recognized, and confused with PEDs in other macular diseases such as typical neovascular age-related macular degeneration (nAMD) and central serous chorioretinopathy (CSC). In the study performed by Liu et al. [16], about half of the eyes with PCV did not show any of the above three typical OCT features for polypoidal lesions. These findings lead us to determine the capacity of these OCT features for identifying the single polypoidal lesion and differentiating from PEDs in other macular diseases.

Optical coherence tomographic angiography (OCTA) is more and more widely used, which allows for visualizing both structure and blood flow in the retina and choroid without any dye injection. As a functional extension of OCT, OCTA provides not only cross-sectional images, but “en face” reconstruction and three-dimensional information of microvasculature. Compared with spectral-domain OCTA (SD-OCTA), which is used in most studies, swept-source OCTA (SS-OCTA) has a longer wavelength and lower sensitivity roll-off, allowing for better penetration through media opacities and retinal pigment epithelium (RPE), and showing more choroidal neovascularization (CNV) details [17–23]. Recently, we investigated the morphologic characteristics of PCV lesions using SS-OCTA (PLEX Elite 9000; Carl Zeiss Meditec, Inc.). All polypoidal lesions appeared as a vascularized PED on cross-sectional images corresponding to a clusters-like structure on en face images after accurate manual segmentation [4]. In this study, we reviewed multiple imaging types of patients with PCV, nAMD, and CSC, to evaluate and compare the diagnostic capability of the above detective

features using SD-OCT and SS-OCTA for differentiating polypoidal lesions from other PED lesions.

Materials and methods

We conducted an observational cross-sectional study including patients who presented to Shanghai General Hospital from December 2017 to August 2019, with diagnosis of serous or serosanguinous maculopathy in unilateral or bilateral eyes, including PCV, typical nAMD, and CSC. Patients underwent all five imaging types including color fundus photography (CFP), SD-OCT, SS-OCTA, fundus fluorescein angiography (FFA), and ICGA at the same visit or within a week without any treatment during this time. Exclusion criteria for the study were (1) coexisting fundus abnormalities such as diabetic maculopathy, uveitis, myopic degeneration, inflammatory disease, and intraocular tumor, (2) poor quality of images for motion artifacts or the presence of optical media opacities including vitreous hemorrhage, dense cataract, and cloudy cornea, and (3) OCTA images with signal strength less than 8. The study was approved by the medical ethics committee of Shanghai General Hospital, and all investigations followed the tenets of the Declaration of Helsinki.

The patients all received a series of baseline ophthalmologic examinations, including CFP (Visucam 200 Digital Fundus Camera; Carl Zeiss Meditec AG), simultaneous FFA and ICGA (Spectralis; Heidelberg Engineering, Inc.), SD-OCT (Spectralis; Heidelberg Engineering), and SS-OCTA (PLEX Elite 9000; Carl Zeiss Meditec, Inc.). The data were collected retrospectively from the medical records including basic demographics, diagnosis, affected eye, the number of intravitreal anti-VEGF injections, and PDT treatments.

Two retinal specialists (HW and FW) reviewed all images to determine the clinical diagnosis of study eyes. The diagnosis of PCV was made based on the EVEREST criteria, including the presence of focal hyperfluorescent spots on ICGA plus at least one of the following: BVN, pulsatile polypoidal lesions, nodular appearance when viewed stereoscopically, hypofluorescent halo, an orange subretinal nodules on fundus photography, or association with massive submacular hemorrhage [24]. The diagnosis of nAMD was made based on FFA findings of classic or occult CNV, without polypoidal lesions or BVN shown on ICGA [25]. The diagnosis of CSC was made based on the presence of a characteristic pattern of leak on FFA-smokestack or inkblot and abnormal dilated choroidal vasculature on ICGA [26].

As for the identification of polypoidal lesions using SD-OCT and SS-OCTA, each of the two prespecified criteria (as detailed below) was graded independently by two trained readers (YW and MS for SD-OCT images; QB and JS for SS-OCTA images) blinded to the clinical diagnosis

and the ICGA findings. In parallel, two other readers (PH and JW) determined the number of polypoidal lesions in each case based on the EVEREST criteria [24]. The detective accuracy of SD-OCT and SS-OCTA is determined based on using ICGA as the gold standard. Disagreement was discussed by open arbitration.

SD-OCT imaging

We focused on localized PEDs in this study. PEDs with the maximum height less than 50 μm and flat irregular PEDs shown as “double-layer sign” were not considered. Two adjacent coalescent PEDs would be considered as a single lesion. The prespecified criterion of polypoidal lesions on SD-OCT was the presence of one of three features including sharply peaked PED, notched PED, and hyperreflective ring surrounding hyporeflective lumen underneath PED [14, 15]. The parameters of all PEDs were measured for analyzing the causes of misdiagnosis. We chose the scans that visualized PEDs with the largest area. The height of PED was manually measured as the maximum distance between the Bruch membrane and the outer boundary of RPE. The base diameter of PED was measured as the distance between the terminations of the RPE elevation using Bruch membrane as the reference plane. The area of PED was the maximum area enclosed by detached RPE and the Bruch membrane. The above parameters were determined using the automated software algorithm of OCT device. Besides, the angle of PED was measured as the greatest angle within all scans on both nasal and temporal sides. The measurement methods are shown in Supplementary Fig. 1. The mean value of these measurements between the two readers was considered for the statistical analysis.

SS-OCTA imaging

SS-OCTA was performed as we previously described [4]. The inner boundary followed the RPE, and the outer boundary followed the Bruch membrane. Manual segmentation strategy was used for each case to optimally visualize the polypoidal lesions. SS-OCTA was reviewed with combined usage of en face and cross-sectional images. The prespecified criterion of polypoidal lesions using SS-OCTA was the presence of vascularized PED on cross-sectional images, with corresponding cluster-like structure at the edge of a BVN on en face images.

Statistical analysis

Baseline demographics and PED parameters were expressed as mean and SD. We performed unpaired *t*-test to compare PED features of polypoidal lesions detected and undetected by using SD-OCT. *P* values of <0.05 were considered statistically significant.

Table 1 Demographic and clinical characteristics of study eyes.

	PCV	Typical nAMD	CSC
Number of affected eyes, <i>n</i>	30	22	20
Age, years [standard derivation]	66.0 [7.8]	69.1 [11.9]	64.5 [12.6]
Gender, male, <i>n</i> , %	19 (63.3)	12 (54.5)	10 (50.0)
Treatment naive, <i>n</i> (%)	15 (50.0)	8 (36.4)	15 (75.0)
Number of PEDs on SD-OCT, <i>n</i>	68	32	28
Number of polypoidal lesions, <i>n</i>			
ICGA	61	0	0
SD-OCT	47	2	0
SS-OCTA	61	6	0

PCV polypoidal choroidal vasculopathy, nAMD neovascular age-related macular degeneration, CSC central serous chorioretinopathy, CNV choroidal neovascularization, PED pigment epithelial detachment, SD-OCT spectral-domain optical coherence tomography, ICGA indocyanine green angiography, SS-OCTA swept-source optical coherence tomographic angiography.

Results

This study included 72 eyes of 66 Chinese patients. The mean age of the study population was 66.7 ± 10.3 years; 37 (56.1%) patients were male and 29 (43.9%) were female. Demographic and clinical characteristics of study eyes are summarized in Table 1.

A total of 128 localized PEDs were detected on SD-OCT. Among them, 61 lesions were defined as polypoidal lesions by the EVEREST criteria, 49 by SD-OCT, and 68 by SS-OCTA (Table 1). The representative images are shown in Figs. 1 and 2. The sensitivity and specificity of the prespecified criteria for polypoidal lesions using SS-OCTA and SD-OCT are shown in Table 2. Typical features of polypoidal lesions on SD-OCT have a limited sensitivity of 73.8% (45/61) and a high specificity of 94.0% (63/67). Combining en face and cross-sectional SS-OCTA provided a higher sensitivity of 96.7% (59/61) than OCT features (Fig. 2).

A total of 16 polypoidal lesions were not identified using SD-OCT features, but 14 of them were detected by SS-OCTA features. For the purpose of exploring the reasons for missed diagnosis, we further analyzed PED parameters of all 61 ICGA-proven polypoidal lesions on SD-OCT. As shown in Table 3, PEDs of undetected polypoidal lesions had lower height, smaller ratio of height to base diameter, less area, and gentler angle. In other words, a part of polypoidal lesions presenting as small dome-shaped PEDs were easily ignored (Fig. 2). Among the PEDs not considered as polypoidal lesions by SD-OCT, the presence of PEDs with heterogeneous internal reflectivity at the end of a double-layer sign was obviously more often in

Fig. 1 The polypoidal lesions detected by both spectral-domain optical coherence tomography (SD-OCT) and swept-source optical coherence tomographic angiography (SS-OCTA). **A, E** Early-phase indocyanine green angiography shows the presence of hyperfluorescent spots (red dotted circles). **B, F** En face SS-OCTA reveals cluster-like structure (yellow arrows) corresponding to the polypoidal lesion at the edge of a BVN. **C, G** Cross-sectional SS-OCTA images show vascularized pigment epithelial detachment (PED). **D, H** A sharply peaked PED and a notched PED are shown on SD-OCT.

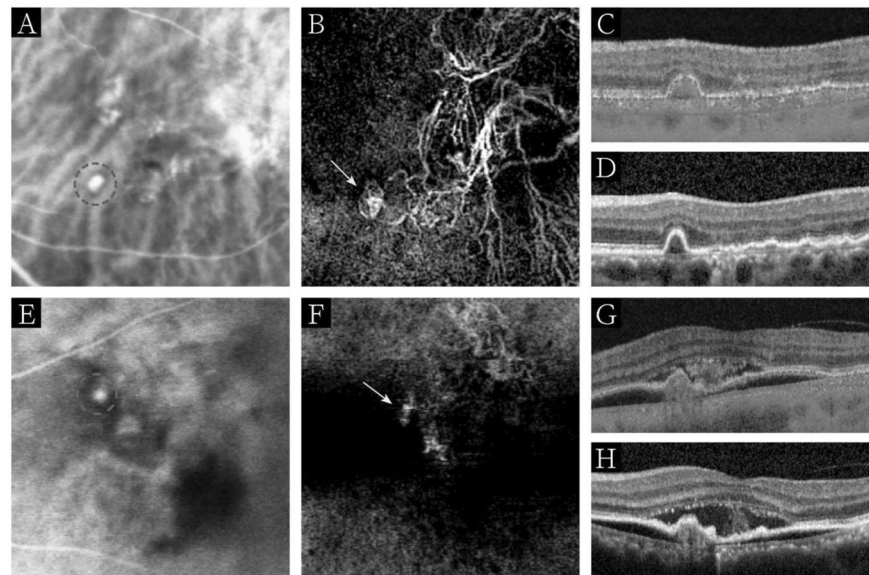


Fig. 2 The polypoidal lesions missed by spectral-domain optical coherence tomography (SD-OCT). **A, E** Early-phase indocyanine green angiography shows the presence of hyperfluorescent spots (red dotted circles). **B, F** En face swept-source optical coherence tomographic angiography (SS-OCTA) reveals a cluster-like structure (yellow arrows) corresponding to the polypoidal lesion at the edge of a BVN. **C, G** Cross-sectional SS-OCTA images show vascularized pigment epithelial detachment (PEDs). **D, H** Small dome-shaped PEDs contiguous with a double-layer sign are shown on SD-OCT.

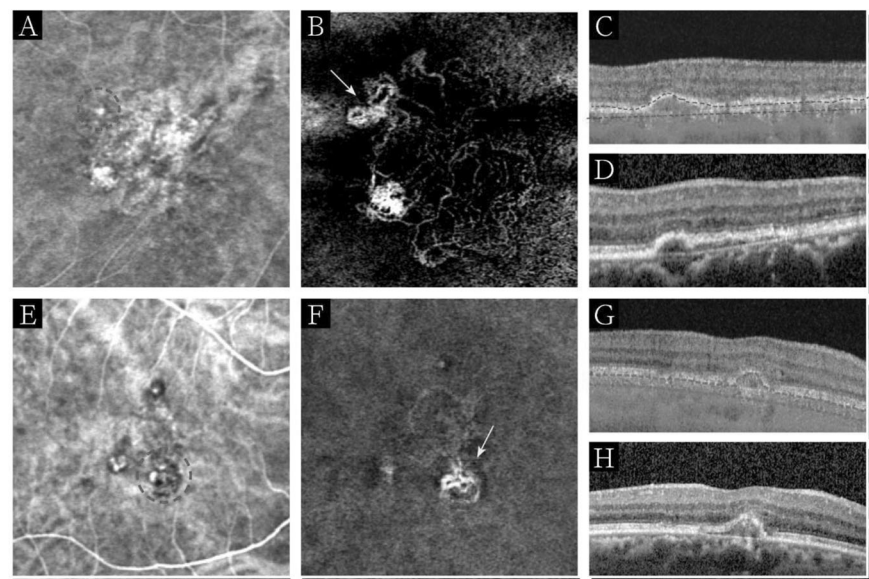


Table 2 Sensitivity and specificity of two imaging types.

Imaging types	Sensitivity (95% CI)	Specificity (95% CI)
SD-OCT	73.8% (0.61–0.84)	94.0% (0.85–0.98)
SS-OCTA	96.7% (0.88–0.99)	82.1% (0.70–0.90)

SD-OCT spectral-domain optical coherence tomography, SS-OCTA swept-source optical coherence tomographic angiography, CI confidence interval.

false-negative lesions (14/16, 87.5%) than true-negative ones (3/63, 3.2%) (Table 4). Therefore, a dome-shaped PED may suggest a polypoidal lesion, if combined with inner reflectivity and a connected double-layer sign.

The PED parameters of the lesions misidentified by SS-OCTA were also measured and compared with those of

Table 3 The parameters of pigment epithelial detachments (PEDs) on spectral-domain optical coherence tomography corresponding to polypoidal lesions.

The parameters of PEDs	OCT (+)	OCT (–)	<i>P</i> value
Height (μm)	158.3 \pm 9.6	122.0 \pm 8.5	<0.05
Base diameter (μm)	323.0 \pm 20.8	332.1 \pm 16.6	0.81
Height/base diameter	0.51 \pm 0.03	0.36 \pm 0.02	<0.0001
Area (mm^2)	0.06 \pm 0.01	0.02 \pm 0.003	<0.05
Angle	74.7 \pm 1.2	62.9 \pm 1.1	<0.0001

OCT optical coherence tomography.

true-positive ones. There was no significant difference in base diameter between the two groups (325.9 \pm 16.4 vs 329.3 \pm 31.0 μm ; $P > 0.1$). However, false-positive lesions showed

smaller ratio of height to base diameter (0.19 ± 0.02) than those of true-positive ones (0.47 ± 0.01) ($P < 0.0001$). Furthermore, we have surprisingly found that some of polypoidal lesions on SS-OCTA (5/12), which were not confirmed by ICGA at baseline, developed and were detected on ICGA at follow-up visits. SS-OCTA showed that the flat vascularized PEDs got sharper or notched on cross-sectional images, and the corresponding cluster-like structures developed into larger size on en face images (Fig. 3).

Discussion

Our current study showed the higher sensitivity of predictive features on SS-OCTA compared with typical OCT features, including sharply peaked PED, notched PED, and a hyperreflective ring underneath PED. A part of polypoidal lesions were missed by SD-OCT for the appearance as small

dome-shaped PEDs, whereas detected by SS-OCTA correctly. PEDs of these unrecognized polypoidal lesions had lower height, smaller ratio of height to base diameter, less area, and gentler angle, but most of them had heterogeneous inner reflectivity and a connected double-layer sign. These findings alert clinicians of paying a close attention to small dome-shaped PEDs at the edge of a double-layer sign, which may suggest polypoidal lesions. Some lesions misidentified by SS-OCTA were at risk of progression to real polypoidal lesions confirmed by ICGA, which implies that flat vascularized PED with corresponding small cluster-like structure at the edge of a BVN may be a preclinical marker of polypoidal lesions and require close follow-up.

PED is a structural separation of the RPE from the underlying Bruch membrane. It is prevalent in three common macular diseases, namely nAMD, PCV, and CSC [27]. Recognition of the specific imaging features of PEDs can facilitate determining the underlying disease. Initially, polypoidal lesions in PCV are thought to show up as sharply peaked PEDs on OCT [28]. Tsujikawa et al. [29] later found that some polypoidal lesions were located at the margin of PED and made a tomographic notch at the elevated RPE. A hyperreflective ring surrounding a hyporeflective space within PED is also a typical feature and probably represents the polypoidal lumen [15]. In our case series, the above features assist us in identifying the majority of polypoidal lesions (73.8%) and excluding almost all non-polypoidal lesions (94.0%).

The polypoidal lesions shown as small dome-shaped PEDs, however, were missed diagnosed. Those unrecognized

Table 4 The features of PEDs not considered as polypoidal lesions by spectral-domain optical coherence tomography.

The features of PEDs	ICGA (+)	ICGA (-)
(A) Heterogeneous internal reflectivity	16/16 (100%)	39/63 (61.9%)
(B) At the end of a double-layer sign	14/16 (87.5%)	10/63 (15.9%)
(C) Both A and B	14/16 (87.5%)	2/63 (3.2%)

PED pigment epithelial detachment, ICGA indocyanine green angiography.

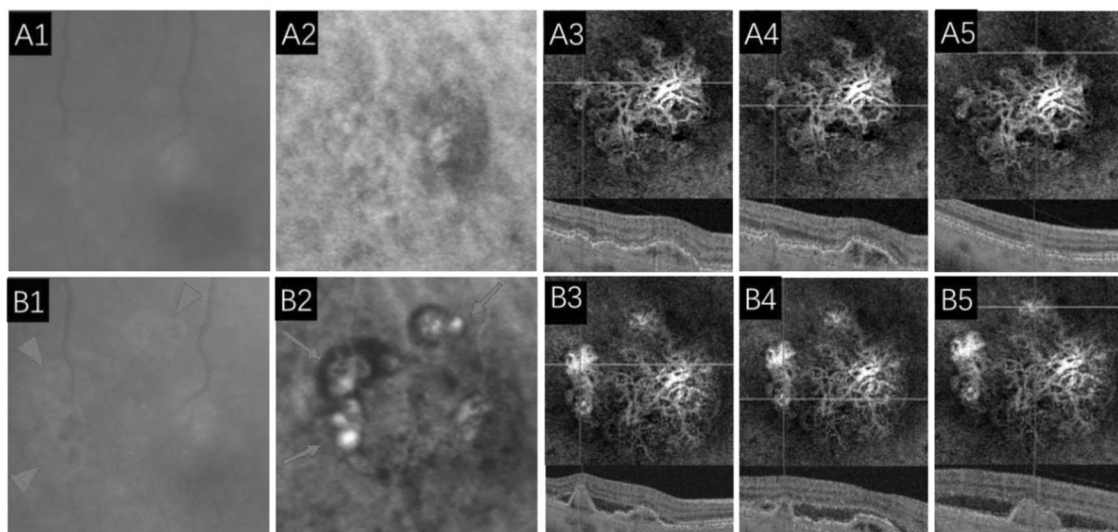


Fig. 3 The incidence of polypoidal lesions in a follow-up patient. **A, B** Show multimodal imaging of first visit and 1-year follow-up evaluation, respectively. **A1, A2** No polypoidal lesions are detected by fundus photography or indocyanine green angiography (ICGA). **A3–A5** The globular structures at the edge of BVN on en face images are small and the relative PEDs are shallow. **B1** Fundus photography

shows three orange–red polypoidal lesions (red arrowheads). **B2** ICGA shows three hyperfluorescent spots surrounded by hypofluorescent ring referring to polypoidal lesions (red arrows). **B3–B5** The globular structures on en face images get larger and tighter, and the pigment epithelial detachments get higher and sharper.

lesions had lower height and area with PEDs, although previous studies suggested that larger PEDs were associated with PCV compared with other PED subtypes [27]. In fact, results from several studies highlight that the greater size of the largest polyp at baseline is related to worse long-term visual outcomes after therapy [7, 8], demonstrating the importance of early detection and management. Besides, the ratio of height to base diameter and the slope of PED have a significant difference between the detected and undetected polypoidal lesions, indicating the incapability of OCT features to identify the polypoidal lesions with flatter structures. Chaikitmongkol et al. [14] defined sharply peaked PED with the angle between 70° and 90°, while we found some polypoidal lesions with an angle less than 70°. These findings made it imperative to rethink the views on characteristic PED features of polypoidal lesions, and notice the probability of missed diagnosis for those showing as small dome-shaped PEDs in clinical practice.

Dome-shaped PEDs appear not only in patients with PCV, but also AMD and CSC [30–32]. Cheong et al. [30] recently found that PED morphology (predominantly dome versus peak) showed no significant difference between nAMD and PCV. There have been other studies that propose the limitation of using OCT parameters to differentiate individual polypoidal lesion from other entities [15, 16]. Thus, how to distinguish the polypoidal lesions from other small dome-shaped PEDs becomes the key to using SD-OCT in this study. We found that compared with true-negative lesions defined by SD-OCT, the missed polypoidal lesions were more likely to appear with heterogeneous internal reflectivity and an associated double-layer sign. Heterogeneous internal reflectivity within PED is commonly thought of as fibrovascular tissue [33, 34], consistent with the description of polypoidal lesions as vascularized PEDs on SD-OCT [27]. A double-layer sign represents a BVN in PCV, and also commonly exists in CSC [32]. Nevertheless, the PED connected to a double-layer sign in patients with CSC is usually serous PED without any internal reflectivity. Based on these findings, we proposed that small dome-shaped PED with heterogeneous internal reflectivity at the edge of a double-layer sign might be an unnoticed feature of polypoidal lesions on OCT images. Note that horizontal scans are acquired routinely in the clinic, but a double-layer sign contiguous with a PED shows on vertical or other directional scans in some cases.

To determine if the PED corresponds to a polypoidal lesion, SS-OCTA images not only provide structural information such as SD-OCT but also visualize the three-dimensional map of microvasculature. We found that most of polypoidal lesions missed by SD-OCT were identified by SS-OCTA (14/16), shown as vascularized PEDs on cross-sectional images and corresponded with a cluster-like structure at the edge of a BVN on en face images. A few

studies have revealed that polypoidal lesions were poorly defined using only en face OCTA [35–38], while localized sub-RPE hyperflow signal on cross-sectional OCTA has a high sensitivity of 69.4–100% [17, 35, 39–41]. In this study, the diagnostic accuracy was high when the features on both en face and cross-sectional images were considered together, which was similar to the results in some other researches [35, 42]. We infer that en face OCTA shows high-resolution spatial relationships of polypoidal lesions and associated vascular networks after identifying the layer and the area of interest, but does not provide stereo information just like ICGA, so polypoidal lesions may not stand out from the associated BVN. When cross-sectional images are reviewed simultaneously, structural and angiographic information along the z-axis is also visualized.

Though prespecified criterion using SS-OCTA had a high sensitivity, SS-OCTA cannot replace ICGA because of the limited specificity. There were false-positive lesions that met the prespecified SS-OCTA criterion but not recognized by ICGA. We found the PEDs of these lesions had smaller ratio of height to base diameter compared with that of true-positive ones. It was an interesting finding that smaller ratio of height to base diameter was not only the characteristic of the lesions missed by SD-OCT, but also of the lesions misidentified by SS-OCTA. Longitudinal changes of false-positive lesions were observed to obtain more information from SS-OCTA. Some of the cluster-like structures developed into ICGA-proven polypoidal lesions at follow-up unexpectedly, and SS-OCTA images displayed the larger cluster-like structures and sharper PEDs with blood flow signal. To date, the exact pathogenesis of the PCV complex remains to be elucidated. Based on this finding, we speculate that patients who presented flat vascularized PEDs and corresponding cluster-like structures at the edge of a BVN on SS-OCTA without ICGA confirmation may be a preclinical PCV and need long-term follow-up. Previous studies have suggested several precursor lesions of PCV, such as large drusen-like deposits, RPE atrophy, and late geographic hyperfluorescence on ICGA [43–45]. SS-OCTA provides a novel and reliable method to investigate the preclinical lesions and pathomechanism of PCV in further research. According to the findings in this study, we infer that the process of some polypoidal lesions formation may be that the twisting of the end of new vessels tangle into a larger cluster-like structure and protrude into the retina. In the study by Fujita et al. [17], it was an interesting finding that small polypoidal lesions appeared as single circular vascular structures on en face OCTA, while the larger ones as tangled or coil-like structures, which might be another indirect evidence of our speculation. In contrast, Chi et al. [5] demonstrated that polypoidal lesions were aneurysm dilation of BVNs and located beneath the roof of the PED. Unlike these findings, several studies revealed that polypoidal lesions could develop development without preexisting type 1 CNV

[43, 46]. Therefore, a longitudinal study with the usage of SS-OCTA is warranted for validation.

Artifacts are an important factor leading to the misinterpretation of OCTA images, commonly including projection, segmentation error, movement, masking, unmasking, and defocus [47, 48]. In the process of using SS-OCTA to detect polypoidal lesions, we found that the presence of PEDs especially bigger ones resulted in segmentation error. We applied the RPE-fit segmentation strategy combined with manual adjust, given polypoidal lesions located between the Bruch membrane and RPE. This segmentation strategy also eliminated the masking artifacts due to hyperreflective material overlying or within the PED [49, 50]. In addition, focal RPE atrophy that accompanied by PED gave rise to unmasking artifacts [49]. It could be partially solved by combining en face and cross-sectional images. Overall, we improved the detection methods and diagnostic criteria to avoid the artifacts due to PEDs.

Our study had many limitations. First, it is a retrospective study with a small sample size. The detective accuracy of the vascularized dome-shaped PED for polypoidal lesions needs to be further confirmed. Also, we are conducting a prospective study to investigate the possibility that polypoidal lesions only identified by SS-OCTA finally progress to ICGA-proven lesions, hoping to illustrate the pathogenesis of polypoidal lesions. Second, the polypoidal lesions in this study were not completely independent due to the presence of several polypoidal lesions in one eye, which means the possibility that once a polypoidal lesion is identified, the others are more likely to be identified. However, SS-OCTA and SD-OCT images of each case were graded by two trained readers and two retinal specialists in a blinded fashion to reduce observer bias.

In conclusion, our findings have shown that typical OCT features of polypoidal lesions are not sensitive enough, and dome-shaped PEDs may also suggest a polypoidal lesion, particularly those with heterogeneous internal reflectivity and a connected double-layer sign. These atypical features should be noticed by clinicians, given that OCT is frequently used imaging at the first and follow-up visit. Although SS-OCTA cannot completely replace ICGA for the limited specificity, it may be a helpful tool to identify preclinical lesions of PCV and clarify the formation of polypoidal lesions for future research.

Summary

What was known before

- Typical features of polypoidal lesions on OCT include sharply peaked PED, notched PED, and a hyperreflective ring underneath PED. The detection rate of polypoidal lesions using OCTA was limited in most previous studies,

but we found that all polypoidal lesions appeared as a vascularized PED on cross-sectional images corresponding to a clusters-like structure on en face images.

What this study adds

- Typical PED features had a limited sensitivity for detecting polypoidal lesions. A small dome-shaped PED with heterogeneous internal reflectivity and a connected double-layer sign on SD-OCT may suggest a polypoidal lesion of PCV. SS-OCTA may be a helpful tool to investigate preclinical PCV and observe the formation of polypoidal lesions.

Funding The study was supported by the National Major Scientific and Technological Special Project for “Significant New Drugs Development” during the Thirtieth Five-year Plan Period (2019ZX09301113); National Natural Science Foundation of China (81730026); National Key R&D Program (2017YFA0105301); Science and Technology Commission of Shanghai Municipality (CTCCR-2016B02, 17411953000, 19495800700); Shanghai Collaborative Innovation Center for Translational Medicine (TM201722); Leaders Training Program of Shanghai Municipality Commission of Health and Family Planning (2018BR10); and Bethune-Langmu eye research fund for the young and middle-aged ophthalmologist (BJ-LM2018001J).

Author contributions YW and QB had full access to all of the data and take responsibility for the integrity of the data and the accuracy of the data analysis. Concept and design: YW, QB, HJ, HW, and FW. Acquisition, analysis, or interpretation of data: YW, QB, HJ, MS, YY, JS, PH, JW, NX, HW, FW, and XS. Drafting of the manuscript: YW, QB, MS, JS, YY, PH, JW, and NX. Critical revision of the manuscript for important intellectual content: HW, FW, and XS. Statistical analysis: YW, QB, and HJ. Obtained funding: PH, FW, and XS.

Compliance with ethical standards

Conflict of interest The authors declare that they have no conflict of interest.

Publisher's note Springer Nature remains neutral with regard to jurisdictional claims in published maps and institutional affiliations.

References

1. Wong CW, Yanagi Y, Lee WK, Ogura Y, Yeo I, Wong TY, et al. Age-related macular degeneration and polypoidal choroidal vasculopathy in Asians. *Prog Retin Eye Res* 2016;53:107–39.
2. Yannuzzi LA, Sorenson J, Spaide RF, Lipson B. Idiopathic polypoidal choroidal vasculopathy (IPCV). *Retina*. 1990;10:1–8.
3. Cheung CMG, Lai TYY, Ruamviboonsuk P, Chen SJ, Chen Y, Freund KB, et al. Polypoidal choroidal vasculopathy: definition, pathogenesis, diagnosis, and management. *Ophthalmology*. 2018; 125:708–24.
4. Bo Q, Yan Q, Shen M, Song M, Sun M, Yu Y, et al. Appearance of polypoidal lesions in patients with polypoidal choroidal vasculopathy using swept-source optical coherence tomographic angiography. *JAMA Ophthalmol*. 2019;137:642–50.

5. Chi YT, Yang CH, Cheng CK. Optical coherence tomography angiography for assessment of the 3-dimensional structures of polypoidal choroidal vasculopathy. *JAMA Ophthalmol.* 2017;135:1310–6.
6. Lorentzen TD, Subhi Y, Sorensen TL. Presenting characteristics and prevalence of polypoidal choroidal vasculopathy in Scandinavian patients with treatment-naïve exudative age-related macular degeneration. *Acta Ophthalmol.* 2018;96:475–80.
7. Koizumi H, Kano M, Yamamoto A, Saito M, Maruko I, Sekiryu T, et al. Afibercept therapy for polypoidal choroidal vasculopathy: short-term results of a multicentre study. *Br J Ophthalmol.* 2015;99:1284–8.
8. Kang HM, Koh HJ, Lee CS, Lee SC. Combined photodynamic therapy with intravitreal bevacizumab injections for polypoidal choroidal vasculopathy: long-term visual outcome. *Am J Ophthalmol.* 2014;157:598–606.e1.
9. Lee YA, Yang CH, Yang CM, Ho TC, Lin CP, Huang JS, et al. Photodynamic therapy with or without intravitreal bevacizumab for polypoidal choroidal vasculopathy: two years of follow-up. *Am J Ophthalmol.* 2012;154:872–80.e2.
10. Uyama M, Wada M, Nagai Y, Matsubara T, Matsunaga H, Fukushima I, et al. Polypoidal choroidal vasculopathy: natural history. *Am J Ophthalmol.* 2002;133:639–48.
11. Cho JH, Park YJ, Cho SC, Ryoo NK, Cho KH, Park SJ, et al. Posttreatment polyp regression and risk of massive submacular hemorrhage in eyes with polypoidal choroidal vasculopathy. *Retina.* 2020;40:468–76.
12. Hope-Ross M, Yannuzzi LA, Gragoudas ES, Guyer DR, Slakter JS, Sorenson JA, et al. Adverse reactions due to indocyanine green. *Ophthalmology.* 1994;101:529–33.
13. Chaikitmongkol V, Khunsongkiet P, Patikulsila D, Ratanasukon M, Watanachai N, Jumroendarasame C, et al. Color fundus photography, optical coherence tomography, and fluorescein angiography in diagnosing polypoidal choroidal vasculopathy. *Am J Ophthalmol.* 2018;192:77–83.
14. Chaikitmongkol V, Kong J, Khunsongkiet P, Patikulsila D, Sachdeva M, Chavengsakongkram P, et al. Sensitivity and specificity of potential diagnostic features detected using fundus photography, optical coherence tomography, and fluorescein angiography for polypoidal choroidal vasculopathy. *JAMA Ophthalmol.* 2019;137:661–7.
15. De Salvo G, Vaz-Pereira S, Keane PA, Tufail A, Liew G. Sensitivity and specificity of spectral-domain optical coherence tomography in detecting idiopathic polypoidal choroidal vasculopathy. *Am J Ophthalmol.* 2014;158:1228–38.e1.
16. Liu R, Li J, Li Z, Yu S, Yang Y, Yan H, et al. Distinguishing polypoidal choroidal vasculopathy from typical neovascular age-related macular degeneration based on spectral domain optical coherence tomography. *Retina.* 2016;36:778–86.
17. Fujita A, Kataoka K, Takeuchi J, Nakano Y, Horiguchi E, Kaneko H, et al. Diagnostic characteristics of polypoidal choroidal vasculopathy based on B-scan swept-source optical coherence tomography angiography and its interrater agreement compared with indocyanine green angiography. *Retina.* 2020;40:2296–303.
18. Ting DS, Cheung GC, Lim LS, Yeo IY. Comparison of swept source optical coherence tomography and spectral domain optical coherence tomography in polypoidal choroidal vasculopathy. *Clin Exp Ophthalmol.* 2015;43:815–9.
19. Novais EA, Adhi M, Moulton EM, Louzada RN, Cole ED, Husvogt L, et al. Choroidal neovascularization analyzed on ultrahigh-speed swept-source optical coherence tomography angiography compared to spectral-domain optical coherence tomography angiography. *Am J Ophthalmol.* 2016;164:80–8.
20. Bartselli G, Bartsch DU, Weinreb RN, Camacho N, Nezgoda JT, Marvasti AH, et al. Real-time full-depth visualization of posterior ocular structures: comparison between full-depth imaging spectral domain optical coherence tomography and swept-source optical coherence tomography. *Retina.* 2016;36:1153–61.
21. Zhang Q, Chen CL, Chu Z, Zheng F, Miller A, Roisman L, et al. Automated quantitation of choroidal neovascularization: a comparison study between spectral-domain and swept-source OCT angiograms. *Invest Ophthalmol Vis Sci.* 2017;58:1506–13.
22. Miller AR, Roisman L, Zhang Q, Zheng F, Rafael de Oliveira Dias J, Yehoshua Z, et al. Comparison between spectral-domain and swept-source optical coherence tomography angiographic imaging of choroidal neovascularization. *Invest Ophthalmol Vis Sci.* 2017;58:1499–505.
23. Cicinelli MV, Cavalleri M, Consorte AC, Rabiolo A, Sacconi R, Bandello F, et al. Swept-source and spectral domain optical coherence tomography angiography versus dye angiography in the measurement of type 1 neovascularization. *Retina.* 2020;40:499–506.
24. Tan CS, Ngo WK, Chen JP, Tan NW, Lim TH, Group ES. EVEREST study report 2: imaging and grading protocol, and baseline characteristics of a randomised controlled trial of polypoidal choroidal vasculopathy. *Br J Ophthalmol.* 2015;99:624–8.
25. Yeung L, Kuo CN, Chao AN, Chen KJ, Wu WC, Lai CH, et al. Angiographic subtypes of polypoidal choroidal vasculopathy in Taiwan: a prospective multicenter study. *Retina.* 2018;38:263–71.
26. Daruich A, Matet A, Dirani A, Bousquet E, Zhao M, Farman N, et al. Central serous chorioretinopathy: recent findings and new physiopathology hypothesis. *Prog Retin Eye Res.* 2015;48:82–118.
27. Tan ACS, Simhae D, Balaratnasingam C, Dansingani KK, Yannuzzi LA. A perspective on the nature and frequency of pigment epithelial detachments. *Am J Ophthalmol.* 2016;172:13–27.
28. Iijima H, Iida T, Imai M, Gohdo T, Tsukahara S. Optical coherence tomography of orange-red subretinal lesions in eyes with idiopathic polypoidal choroidal vasculopathy. *Am J Ophthalmol.* 2000;129:21–6.
29. Tsujikawa A, Sasahara M, Otani A, Gotoh N, Kameda T, Iwama D, et al. Pigment epithelial detachment in polypoidal choroidal vasculopathy. *Am J Ophthalmol.* 2007;143:102–11.
30. Cheong KX, Grewal DS, Teo KYC, Gan ATL, Jaffe GJ, Cheung GCM. The relationship between pigment epithelial detachment and visual outcome in neovascular age-related macular degeneration and polypoidal choroidal vasculopathy. *Eye (Lond).* 2020;34:2257–63.
31. Sato T, Iida T, Hagimura N, Kishi S. Correlation of optical coherence tomography with angiography in retinal pigment epithelial detachment associated with age-related macular degeneration. *Retina.* 2004;24:910–4.
32. Yang L, Jonas JB, Wei W. Optical coherence tomography-assisted enhanced depth imaging of central serous chorioretinopathy. *Invest Ophthalmol Vis Sci.* 2013;54:4659–65.
33. Zayit-Soudry S, Moroz I, Loewenstein A. Retinal pigment epithelial detachment. *Surv Ophthalmol.* 2007;52:227–43.
34. Kang H, Byeon SH, Kim SS, Koh HJ, Lee SC, Kim M. Combining en face optical coherence tomography angiography with structural optical coherence tomography and blood flow analysis for detecting choroidal neovascular complexes in pigment epithelial detachments. *Retina.* 2019;39:1551–61.
35. Inoue M, Balaratnasingam C, Freund KB. Optical coherence tomography angiography of polypoidal choroidal vasculopathy and polypoidal choroidal neovascularization. *Retina.* 2015;35:2265–74.
36. Cheung CMG, Yanagi Y, Mohla A, Lee SY, Mathur R, Chan CM, et al. Characterization and differentiation of polypoidal choroidal vasculopathy using swept source optical coherence tomography angiography. *Retina.* 2017;37:1464–74.

37. Cheung CMG, Yanagi Y, Mohla A, Lee SY, Mathur R, Chan CM, et al. Comparison of indocyanine green angiography and optical coherence tomographic angiography in polypoidal choroidal vasculopathy. *Eye (Lond)*. 2017;31:45–52.
38. Tanaka K, Mori R, Kawamura A, Nakashizuka H, Wakatsuki Y, Yuzawa M. Comparison of OCT angiography and indocyanine green angiographic findings with subtypes of polypoidal choroidal vasculopathy. *Br J Ophthalmol*. 2017;101:51–5.
39. Wang M, Zhou Y, Gao SS, Liu W, Huang Y, Huang D, et al. Evaluating polypoidal choroidal vasculopathy with optical coherence tomography angiography. *Invest Ophthalmol Vis Sci*. 2016;57:OCT526–32.
40. Chan SY, Wang Q, Wang YX, Shi XH, Jonas JB, Wei WB. Polypoidal choroidal vasculopathy upon optical coherence tomographic angiography. *Retina*. 2018;38:1187–94.
41. Cheung CM, Laude A, Wong W, Mathur R, Chan CM, Wong E, et al. Improved specificity of polypoidal choroidal vasculopathy diagnosis using a modified EVEREST criteria. *Retina*. 2015;35:1375–80.
42. de Carlo TE, Kokame GT, Kaneko KN, Lian R, Lai JC, Wee R. Sensitivity and specificity of detecting polypoidal choroidal vasculopathy with en face optical coherence tomography and optical coherence tomography angiography. *Retina*. 2019;39:1343–52.
43. Kim YT, Kang SW, Chung SE, Kong MG, Kim JH. Development of polypoidal choroidal vasculopathy in unaffected fellow eyes. *Br J Ophthalmol*. 2012;96:1217–21.
44. Ueta T, Iriyama A, Francis J, Takahashi H, Adachi T, Obata R, et al. Development of typical age-related macular degeneration and polypoidal choroidal vasculopathy in fellow eyes of Japanese patients with exudative age-related macular degeneration. *Am J Ophthalmol*. 2008;146:96–101.
45. Kang SW, Lee H, Bae K, Shin JY, Kim SJ, Kim JM, et al. Investigation of precursor lesions of polypoidal choroidal vasculopathy using contralateral eye findings. *Graefes Arch Clin Exp Ophthalmol*. 2017;255:281–91.
46. Baek J, Cheung CMG, Jeon S, Lee JH, Lee WK. Polypoidal choroidal vasculopathy: outer retinal and choroidal changes and neovascularization development in the fellow eye. *Invest Ophthalmol Vis Sci*. 2019;60:590–8.
47. Holmen IC, Konda SM, Pak JW, McDaniel KW, Blodi B, Stepien KE, et al. Prevalence and severity of artifacts in optical coherence tomographic angiograms. *JAMA Ophthalmol*. 2020;138:119–26.
48. Spaide RF, Fujimoto JG, Waheed NK. Image artifacts in optical coherence tomography angiography. *Retina*. 2015;35:2163–80.
49. Tan ACS, Freund KB, Balaratnasingam C, Simhaee D, Yannuzzi LA. Imaging of pigment epithelial detachments with optical coherence tomography angiography. *Retina*. 2018;38:1759–69.
50. Chen L, Zhang X, Gan Y, Liu B, Zhang Y, Wen F. Retinal pigment epithelium hyperplasia overlying pigment epithelial detachment in age-related macular degeneration can masquerade as neovascularization on optical coherence tomography angiography. *Graefes Arch Clin Exp Ophthalmol*. 2018;256:2283–91.